Mechanical Properties of Bioplastics and Bioplastic–Organoclay Nanocomposites Prepared from Epoxidized Soybean Oil with Different Epoxide Contents

Varaporn Tanrattanakul, Pimchanok Saithai

Bioplastic Research Unit, Polymer Science Program, Faculty of Science, Prince of Songkla University, Hatyai, Songkla 90112, Thailand

Received 21 January 2009; accepted 22 March 2009
DOI 10.1002/app.30842
Published online 28 July 2009 in Wiley InterScience (www.interscience.wiley.com).

ABSTRACT: The objectives of this study were to investigate the effect of epoxide content (24–88 mol %) on the mechanical properties and characteristics of epoxidized soybean oil (ESO) and to compare the mechanical properties of ESO–organoclay nanocomposites with different epoxide contents (40 and 100 mol %). ESO was synthesized by *in situ* epoxidation with acetic acid and hydrogen peroxide. We prepared ESO bioplastic sheets from ESO by curing with methyltetrahydrophthalic anhydride and 1-methylimidazole. The tensile properties and tear resistance of the synthesized bioplastic (ESO40, where the number indicates the molar percentage of epoxidation) were investigated and compared with ESO bioplastic sheets prepared from commercial ESO with 100 mol % epoxidation (ESO100). The tensile modulus, tensile strength, tensile toughness, and tear strength of the ESO bioplastics increased with increasing epoxide content, whereas the elongation at break of the ESO100 bioplastic was lowest. No trend was observed in the bioplastics prepared from ESO24–ESO88. Dynamic mechanical thermal analysis showed increases in the storage modulus and glass-transition temperature as the epoxide content was increased. Thermal degradation also increased with increasing epoxide content. The crosslink density and chain flexibility controlled the mechanical properties and characteristics of the ESO bioplastics. ESO–organoclay nanocomposites were prepared by *in situ* intercalative polymerization. The addition of organoclay increased the mechanical properties of the ESO bioplastics. The effect of organoclay content (1–8 wt %) on the mechanical properties was similar to the effect of the epoxide content. The sESO100 nanocomposite showed a higher modulus but lower tensile strength and elongation at break than the ESO40 nanocomposite. Intercalation of the organoclay in the ESO nanocomposites was observed by transmission electron microscopy and X-ray diffractometry. © 2009 Wiley Periodicals, Inc. J Appl Polym Sci 114: 3057–3067, 2009

Key words: biopolymers; clay; crosslinking; mechanical properties; nanocomposites

INTRODUCTION

Recently, the industrial sectors and researchers have paid more attention to biobased plastics for many reasons. For example, raw materials produced from petrochemicals are becoming more and more expensive because of the increase in oil price and the lower supply. With greater public demand for environmentally friendly products and greater concern about global warming, problems arising from conventional plastic production are becoming an important issue. As a result, plastics from renewable agricultural products are being developed and will become the next generation of plastic materials. Soybean oil (SO) is one of the raw materials with a high potential for new bioplastics. Modified SO is a promising alternative in many applications, including plastic sheet-molding compounds, coatings, and adhesives.[1] The synthesis of epoxidized soybean oil (ESO) was already been patented[2–4] and published.[5] ESO with 100 mol % epoxidation (ESO100) was commercialized under various trade names and is used in lubricant application and as a plasticizer of poly (vinyl chloride). Until now, many researchers have worked on the chemical modification and new applications of ESO. The degradation of the epoxide ring in ESO was studied by Campeanella and Baltanas.[6,7] The chemical modification of ESO by the ring opening of the epoxide ring has been widely studied to obtain new products, including polyol,[8,9] lubricant additive,[10] synthetic lubricant,[11] SO–styrene–divinylbenzene copolymer,[12,13] SO monoglyceride maleate–polystyrene copolymer[14] and epoxy methyl esters.[15]

Correspondence to: V. Tanrattanakul (varaporn.t@psu.ac.th).

Contract grant sponsor: Research, Development, and Engineering Fund (through the National Nanotechnology Center).

Contract grant sponsor: National Science and Technology Development Agency of Thailand; contract grant number: NN-B-22-CT2-19-50-07.

Contract grant sponsor: Graduate School of Prince of Songkla University.

© 2009 Wiley Periodicals, Inc.

ESO has been used on its own as a PVC plasticizer,[16] in coatings (without other polymers),[17,18] and in coatings with other polymers, including terpinolene resin,[19] epoxy resin,[20] and styrene/acrylic copolymer.[21] Polyurethane foam was synthesized with polyol derived from modified ESO.[22] Because of the flexible hydrocarbon backbone, ESO was used as a toughening agent for thermosetting plastics, including phenolic resins[23,24] and epoxy resin.[25–29] The high reactivity of the epoxide ring makes ESO able to crosslink with a suitable hardener. The so-called bioplastic could be applied to thermosetting derived from crosslinked ESO. Sheet-molding compound resins prepared from acrylated ESO have been reported.[30,31] The viscoelastic properties of crosslinked ESO have been studied in terms of effects of different curing agents[32] and hydrogel properties.[33] Although ESO nanocomposites are very interesting because the *in situ* intercalation can be easily prepared, not many studies have been reported in this field. Titanium(IV) oxide anatase with a particle size of 32 nm was mixed in ESO.[34] There are a few publications reporting nanocomposites prepared from organoclay and ESO.[35–37] Organoclay was also used in ESO–polymer blends. For example, Liu and Erhan[38] prepared organoclay nanocomposites of epoxy/ESO blends. Lu and Wool[39] used organoclay to reinforce ESO liquid rubber blended with polystyrene. The organoclay frequently used in those studies was Cloisite 30B, and the curing agent frequently used was triethylenetetramine. Additionally, the ESO used in all of the previous studies was a commercial grade containing 100 mol % epoxidation (ESO100). No mechanical properties of ESO or ESO nanocomposites containing epoxide contents of less than 100 mol % were reported. The commercial ESO100 may not be suitable for the preparation of bioplastics because of high brittleness. The new approach is to seek new ESOs that provide higher ductility or toughness. Therefore, it is necessary to develop new ESOs containing various epoxide contents and determine their mechanical properties and characteristics. ESO–organoclay nanocomposites should be extensively researched to obtain better mechanical properties.

The aims of this study were to investigate the effect of epoxide content (24–88 mol %) on the mechanical properties of ESO bioplastics and to develop bioplastic nanocomposites from ESO containing 40 mol % epoxidation and organoclay via *in situ* intercalative polymerization. In this study, the organoclay used was different from that used in all of the previous studies. The polymer characterization and morphology of bioplastics and bioplastic nanocomposites are discussed as well. The mechanical properties of synthesized ESO bioplastics and ESO–organoclay nanocomposites were compared to those of samples prepared from commercial ESO (ESO100). The possible applications of these new bioplastics and bioplastic–organoclay nanocomposites are sheets or films.

EXPERIMENTAL

Materials

Commercial food-grade SO produced by Thai Vegetable Oil Public Company Limited (Bangkok, Thailand) was purchased from a supermarket and was used without further purification. Glacial acetic acid (Labscan Co., Ltd., Gliwice, Poland), 30% v/v hydrogen peroxide (Merck, Darmstadt, Germany), and sulfuric acid (Labscan Asia Co., Ltd., Bangkok, Thailand) were used for the *in situ* epoxidation. Anhydrous sodium sulfate (Fischer Scientific, Pittsburgh, PA) was used for the dehydration process after synthesis. Chloroform (Labscan Co., Ltd., Gliwice, Poland) was used as a solvent for ESO. All of the chemicals used were analytical grade. The Vikoflex 7170 (100 mol % epoxidation, 7% oxirane oxygen) produced by Arkema, Inc. (Philadelphia, PA) was used as the reference oil. Bentonite-based organoclays included Bengel 434 [trimethylalkyl (C14–20) ammonium bentonite] produced by Elements Specialties, Inc. (Hightstown, NJ) and octadecyl trimethyl (C16) ammonium bentonite (OTAC). The chemical structure of the surfactant is displayed in Figure 1(a), whereby the number of carbons (n) in trimethylalkyl ammonime and ocadecyl trimethyl ammonium were 14–20 and 16, respectively. Bentonite (montmorillonite) is commonly used as a layered silicate in polymer–clay nanocomposites. Its crystal structure, as shown in Figure 1(b), is characterized by a 1 nm thick silicate layer consisting of two silica tetrahedral sheets fused to an edge-shared octahedral sheet of nominally Al, Fe, Mg, or Li. Between each silicate layer, it consists of exchangeable cations, for example, Li^+, Na^+, Rb^+, or Cs^+. The gap between each layer is called a *gallery* or *interlayer*. Methyltetrahydrophthalic anhydride (MTHPA; Lindried 46QC, produced by Lindau Chemicals Co., Columbia, SC) and 1-methylimidazole (Sigma-Aldrich, St. Louis, MO) were used as a curing agent and a catalyst, respectively, for the curing reaction. Deuterated chloroform ($CDCl_3$; 99.8% D; SP Industries Co., Warminster, PA) was used as a solvent for investigation by NMR. All chemicals were used as received.

Preparation and characterization of ESO

The *in situ* epoxidation of SO was carried out with hydrogen peroxide and acetic acid. The molar ratio of SO to acetic acid to hydrogen peroxide to sulfuric

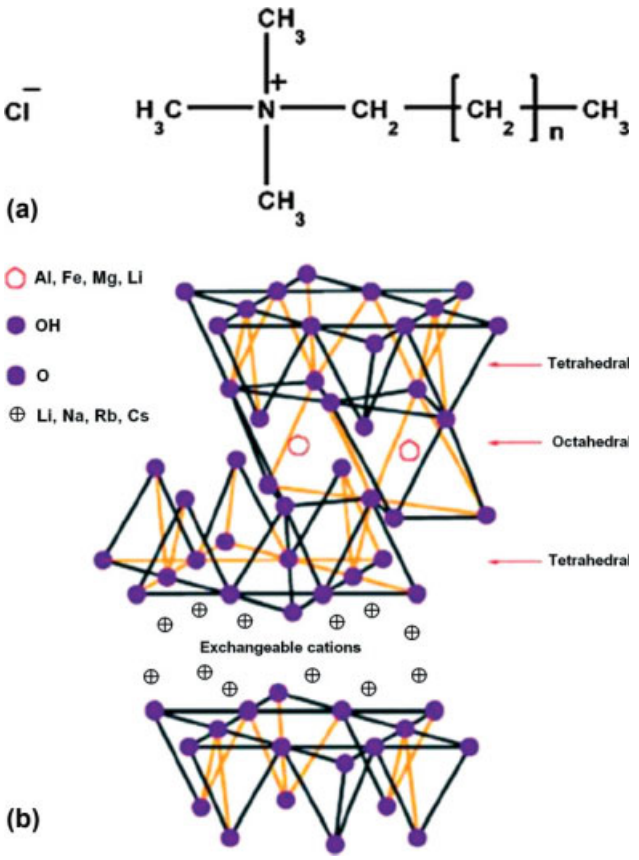

Figure 1 Chemical structures of (a) the surfactants and (b) bentonite. [Color figure can be viewed in the online issue, which is available at www.interscience.wiley.com.]

acid was 1 : 3 : 5 : 0.009. The average molecular weight of the SO used was 871.79 g/mol, which was characterized by gas chromatography (6850, Hewlett Packard, Ramsey, MN) with an average functionality of 4.6 carbon–carbon double bonds per triglyceride. Our obtained molecular weight was similar to that of other SOs.[30,40] Sulfuric acid acted as a catalyst for the epoxidation reaction. SO was added to the reactor when the temperature of the water bath reached 55°C. Acetic acid and sulfuric acid were added dropwise in the SO under continuous stirring. Hydrogen peroxide was slowly dripped for approximately 20–30 min. The reaction temperature was maintained at 55 ± 2°C throughout the reaction period (5–8 h). The epoxidation reaction was terminated by the cooling of the reactor. ESO was neutralized by distilled water until the pH of the mixture was 7. Water was removed with a separating funnel, and sodium sulfate anhydrous was added to the ESO sample for dehydration. After filtration, the degree of epoxidation was determined by ^{1}H-NMR spectroscopy (Varian Unity Inova 500 MHz, Palo Alto, CA). The epoxide content was calculated with eq. (1):[41–43]

$$\text{Epoxide content (mol\%)} = \frac{I_{3.0-3.15}}{I_{3.0-3.15} + I_{5.3-5.6}} \quad (1)$$

where $I_{3.0–3.15}$ and $I_{5.3–5.6}$ are the integrated values of the peaks at δ = 3.0–3.15 ppm (epoxy proton) and δ = 5.3–5.6 ppm (C**H**=C**H**), respectively.[5,10] The peak at δ = 2.8–3.0 ppm belonged to the C**H**$_2$ proton adjacent to two epoxy groups.[10] The nomenclature of the ESO sample is based on the epoxide content; for example, ESO40 or ESO100 represent epoxide contents of 40 and 100 mol %, respectively. SO and ESOs were also characterized by Fourier transform infrared (FTIR) spectroscopy (Equinox 58, Bruker, Billerica, MA).

Preparation of the ESO–organoclay nanocomposites

Two different kinds of organoclays were selected for this study: Bengel 434 and OTAC. It is not the aim of this article to report the synthesis method and characteristics of the organoclays. Nanocomposites containing Bengel 434 and OTAC were prepared by the following method. The organoclay was dried in a vacuum oven (model 29, Precision, Munich, Germany) at 105°C for 24 h before use. The organoclay was dispersed in chloroform with an ultrasonic device at a frequency of 60 kHz for 4 h. The required amount of organoclay dispersion was added in ESO under continuous stirring with a magnetic bar. The mixture of ESO and organoclay was sonicated again for 4 h. Chloroform was eliminated with a rotary evaporator (Rotavapor R-200, Buchi, St. Gallen, Switzerland). The ESO organoclay mixtures were vacuum-dried at 60°C for 24 h and kept in sealed bottles.

Preparation of the ESO bioplastic sheets and ESO nanocomposite sheets

All of the samples of ESO and mixtures of ESO and organoclay, except ESO100 mixed with Bengel 434, were mixed with 60 parts per hundred of ESO by weight (pphr) of MTHPA and 1-pphr 1-methylimidazole. The curing temperature and time were 150°C and 75 min, respectively. The curing process was performed in an oven (UFB400, Memmert, Schwabach, Germany). Because of the appearance of the cured sheets obtained from ESO100 mixed with Bengel 434, it was necessary to change the chemical composition and curing conditions. The appropriate chemical composition became 40-pphr MTHPA and 1-pphr 1-methylimidazole, and the curing conditions were 135°C and 60 min.

Mechanical property testing and characterization

The die-cut specimens were prepared from the sheet samples. The tensile properties (ASTM D 412C) and

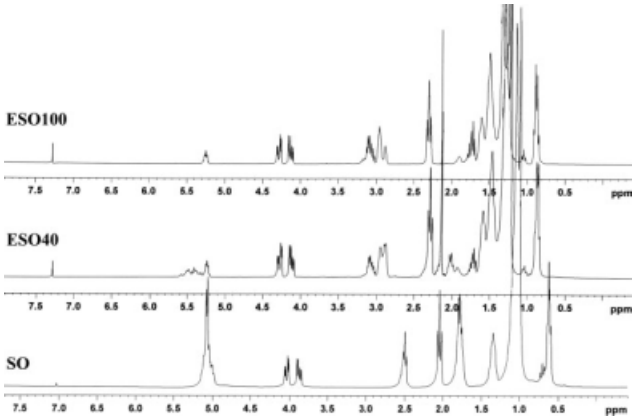

Figure 2 NMR spectra of SO (bottom), ESO40 (middle), and ESO100 (top).

tear strength (ASTM D 624, the right-angle specimen) were determined with a universal testing machine (Instron 5569, Norwood, MA) with a crosshead speed of 50 mm/min. The gauge length of the tensile testing specimen was 35 mm. Testing was carried out at 25°C, and five specimens were tested for every sample. The dynamic mechanical thermal properties were investigated by a Rheometric Scientific DMTA V (Piscataway, NJ) under tension mode with a strain control of 0.01% at a frequency of 1 Hz, and temperature scans were run from −50 to 80°C at a heating rate of 2°C/min. The presence of nonreacted functional groups in the ESO bioplastic sheets were characterized with a differential scanning calorimeter (DSC7, PerkinElmer, Norwalk, CT) at a heating rate of 10°C/min from 30 to 300°C. Fresh ESO mixed with MTHPA and 1-methylimidazole was used to obtain the complete heat of reaction (ΔH, heat of reaction = 100%). Thermogravimetric analysis (TGA 7, PerkinElmer, Norwalk, CT) was operated at a heating rate of 10°C/min from 50 to 550°C under a nitrogen atmosphere. The characteristics of the organoclay in the ESO nanocomposites were explored by an X-ray diffractometer (D5005, Seimen, Munich, Germany) with Cu Kα radiation (λ = 1.54 Å) at 40 kV/40 mA. The diffractograms were scanned in a 2θ range of 1–10° at a rate of 0.4°/min. The ultramicrotomed sections were prepared at −110°C for microscopy. Transmission electron microscopy (TEM; JEM2010, JEOL, Tokyo, Japan) was applied at an accelerating voltage of 160 kV, and images were recorded at 100,000× magnification.

RESULTS AND DISCUSSION

Determination of the prepared ESO

Figure 2 shows the ^{1}H-NMR spectra of SO, ESO40, and ESO100. The δ assignment of characteristic protons in SO and ESO was reported by Adhvaryu and Erhan[10] and Li and Larock.[12] The ^{1}H-NMR spectra in this study were similar to those reported by those authors. The important chemical shifts of regular SO included the following peaks: 5.0–5.3 ppm (vinylic hydrogens, —C**H**=C**H**—, and methine protons of the backbone, —CH_2—C**H**—CH_2—), 4.0–4.4 ppm (methylene protons, C$\mathbf{H}_2$—CH—C$\mathbf{H}_2$), and 2.4–2.6 ppm (protons in the C$\mathbf{H}_2$ groups between two carbon–carbon double bonds, =CH—C$\mathbf{H}_2$—CH=), whereas the important chemical shifts of ESO40 included the following peaks: 5.3–5.6 ppm (—C**H**=C**H**—), 5.2–5.3 ppm (—CH_2—C**H**—CH_2—), 4.0–4.4 ppm (C$\mathbf{H}_2$—CH—C$\mathbf{H}_2$), 3.0–3.2 ppm (—C**H**— proton of the epoxide ring), and 2.8–3.0 ppm (C$\mathbf{H}_2$ proton adjacent to two epoxide rings). The appearance of the peaks at 2.8–3.2 ppm in ESO40 and ESO100 proved the presence of epoxide ring. Furthermore, the peak height at 5.3–5.6 ppm decreased in ESO40 and disappeared in ESO100; this supported the degree of epoxidation in the samples. On the basis of determination from ^{1}H-NMR spectra, 24–88 mol % epoxide contents were obtained in this study. Epoxide ring opening in the ESO was determined by infrared spectroscopy, and no OH group was detected. As demonstrated in Figure 3, qualitative FTIR investigation showed the epoxide group at a wave number of 824–843 cm^{-1} in ESO40 and ESO100, and only SO showed a sharp peak at 3010 cm^{-1}; this represented the double bond (C=C) of triglyceride.[25] We successfully synthesized ESO containing different epoxidations without a ring-opening side reaction.

Tensile properties and characteristics of ESO bioplastics

The notion of this study was to use the minimum amount of curing agent needed to prevent too much crosslinking and the presence of chemical residue. To formulate the chemical composition, a preliminary study was executed. ESO40 was selected to

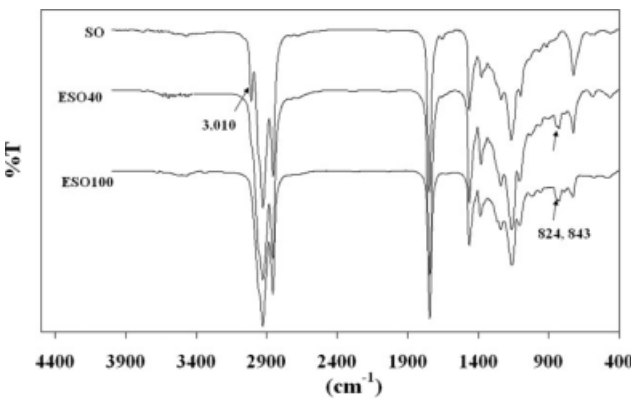

Figure 3 FTIR spectra of SO (top), ESO40 (middle), and ESO100 (bottom).

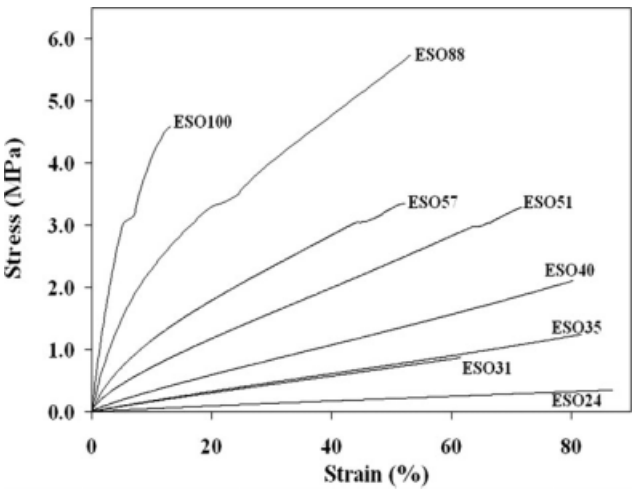

Figure 4 Stress–strain curves of ESO bioplastics with 60 pphr MTHPA cured at 150°C for 75 min.

investigate the effect of the curing agent content. The minimum concentration of MTHPA was 50 pphr to obtain an acceptable sheet in terms of appearance and mechanical properties, and 60-pphr MTHPA provided the optimum tensile properties. Thus, 60-pphr MTHPA was used for all of the samples. The ESO bioplastics in this study were thermoset, and the structure of triglyceride did not support crystallization. Therefore, the mechanical properties of the ESO bioplastics came from the crosslink density, which was the result of the crosslinking reaction between the epoxy ring and MTHPA.

The stress–strain curves and tensile properties of the ESO bioplastics with various epoxide contents are displayed in Figure 4 and Table I, respectively. A brittle fracture manner was obtained. These ESO bioplastics exhibited tensile behavior similar to a conventional synthetic rubber with a low modulus and tensile strength and a moderate elongation at break. All specimens showed rubber elasticity; they snapped back to the original length after failure, except for ESO100, which was very brittle. Nonlinearity in the stress–strain curves was observed in the samples that contained epoxide contents of 51 mol % or greater. The linearity and nonlinearity involved the crosslink density; this was similar to work done by Li and Larock.[13] The linearity in ESO24 to ESO40 was due to less crosslinking in comparison with ESO51 to ESO100. Nonlinearity is usually associated with plastic flow in the sample (plastic deformation). Linearity was related to the flexibility and hardness of the ESO bioplastics. The hardness of these ESO bioplastics was in the range 11–96 Shore A from ESO24 to ESO100. Triglyceride consists of short-chain molecules of three fatty acids. To be a polymer, it needs chemical crosslinking. Although all of the samples were polymers, unfortunately, their molecular weights could not be determined. We believe that the crosslink density and flexibility played an important role in differences in the linearity of these ESO bioplastics. The Young's modulus, tensile strength, and tear resistance increased with increasing epoxide content, which resulted from an increase in the crosslink density. For the elongation at break of the ESO31 to the ESO88 bioplastics, no trend was observed. However, these ESO bioplastics showed a much higher elongation at break than the ESO100 bioplastic, particularly, the ESO40 bioplastic, which showed the highest elongation at break. When the epoxide content increased, crosslinking in ESO was enhanced, which led to a more rigid structure and less segmental mobility. The tensile toughness was obtained from the area under the stress–strain curves, as exhibited in Figure 4. The tensile toughness increased with increasing epoxide content from 24 to 88 mol % and then decreased when the epoxidation was 100 mol %, as listed in Table I. The ESO100 bioplastic showed the most brittleness and a very low elongation at break; therefore, the tensile toughness was lowest, although the modulus was very high. These results suggest that the improvement in the toughness of the ESO100 bioplastic was well done in this study by the decrease in the epoxide content, as mentioned in the previous assumption.

TABLE I
Effect of the Epoxide Content on the Tensile Properties and Tear Strength of the ESO Bioplastics with 60-pphr MTHPA Cured at 150°C for 75 min

Epoxide content (mol %)	Modulus (MPa)	Tensile strength (MPa)	Elongation at break (%)	Tear strength (N/mm)	Tensile toughness (MPa)
24	0.70 ± 0.04	0.39 ± 0.04	98 ± 10	0.87 ± 0.11	0.17 ± 0.00
31	1.97 ± 0.11	0.80 ± 0.05	58 ± 4	2.18 ± 0.19	0.29 ± 0.01
35	2.19 ± 0.22	1.05 ± 0.19	66 ± 11	2.30 ± 0.48	0.52 ± 0.01
40	2.74 ± 0.29	1.33 ± 0.14	78 ± 6	2.85 ± 0.30	0.89 ± 0.01
51	4.79 ± 0.40	1.88 ± 0.35	69 ± 13	3.56 ± 0.23	1.34 ± 0.00
57	17.04 ± 2.07	3.35 ± 0.53	59 ± 6	4.48 ± 0.91	1.08 ± 0.01
88	20.81 ± 2.15	3.75 ± 0.32	53 ± 8	4.98 ± 0.27	1.94 ± 0.02
100	37.71 ± 7.70	5.75 ± 0.90	15 ± 5	5.72 ± 1.11	0.42 ± 0.01

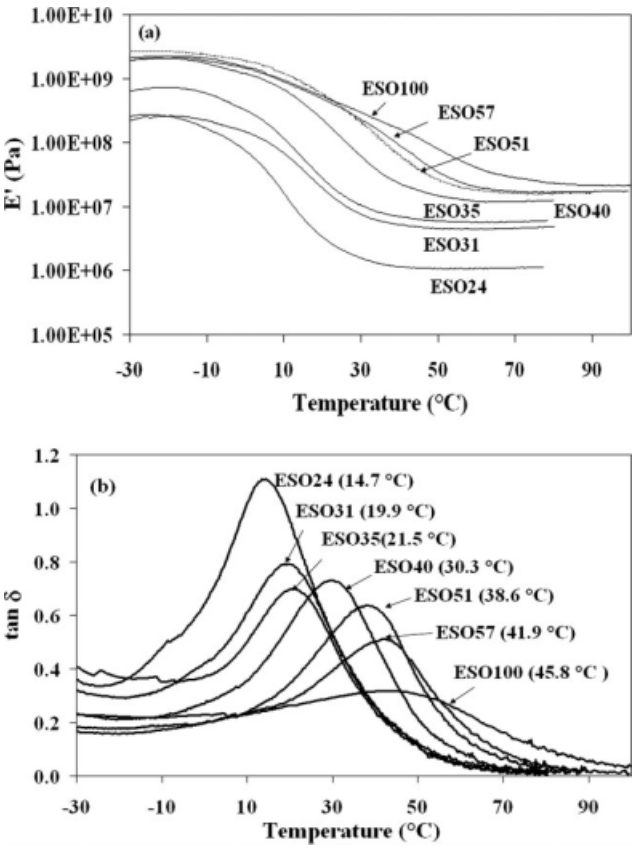

Figure 5 DMTA traces of ESO bioplastics with different epoxide contents: (a) E' and (b) tan δ.

Figure 5 shows the temperature dependence of the storage modulus (E') and the loss factor (tan δ) for all of the ESO bioplastics. E' increased with increasing epoxide content, similarly to Young's modulus. The modulus in the rubbery plateau region also increased with epoxide content. This modulus relates to crosslink density on the basis of the theory of rubber elasticity, as written in eq. (2):

$$E' = 3nRT \tag{2}$$

where E' is the storage modulus in the rubbery plateau region, n is the crosslink density, R is the gas constant, and T is the absolute temperature at the rubbery plateau region, generally 30–50°C above the α-relaxation temperature. The rubbery modulus at 70°C was selected to calculate the crosslink density for all of the ESO bioplastics except the ESO100 bioplastic, whereby the rubbery modulus was calculated at 90°C. The calculated values of crosslink density increased with increasing epoxide content in the range 131–2610 mol/m^3 from the ESO24 bioplastic to the ESO100 bioplastic. This result substantiates the hypothesis that crosslink density increased with epoxide content.

All of the ESO bioplastics showed a broad transition from the glassy to the rubbery state because of the plasticizing characteristics of saturated fatty acids in the network.[30] The temperature shown in Figure 5(b) was the temperature at the maximum tan δ, which was in the range 14.7–45.8°C from the ESO24 bioplastic (14.7°C) to the ESO100 bioplastic (45.8°C). Park et al.[5] prepared a bioplastic sheet from ESO100 polymerized with *N*-benzylpyrazinium hexafluoroamtimonate, and the glass-transition temperature (T_g) determined from the tan δ peak was 24°C, which was lower than that derived in this study. This was because of the differences in the curing agent type and concentration, although a shorter curing time was used in this study. It is known that the temperature at the maximum tan δ is equivalent to T_g of the polymer and T_g derived from dynamic mechanical thermal analysis (DMTA) is different from that derived from DSC. It has been stated that for most thermosetting plastics, the tan δ peak at a frequency of 1 Hz generally occurs at a temperature of 15–20°C above T_g, as measured by dilatometry or differential thermal analysis.[30] Therefore, such T_g's of the ESO bioplastics were approximately 30°C for the ESO100 bioplastic, 15°C for the ESO40 bioplastic, and 0°C for the ESO24 bioplastic.

To verify the presence of unreacted functional groups in the ESO bioplastics, sample sheets were characterized with DSC. No exothermic peak due to the crosslinking reaction occurring during the heating scan was observed; this suggested that all of the epoxide rings reacted with MTHPA. The decomposition temperatures of the ESO bioplastics obtained from TGA (listed in Table II) were determined for 5, 10, and 50% weight losses (T_5, T_{10}, and T_{50}, respectively). The abrupt weight loss occurred after T_{10}. The effect of the epoxide content at each decomposition temperature was different. T_5 and T_{10} tended to increase with increasing epoxide content from 24 to 57 mol %, whereas the T_{50} values of all of the samples were similar. All of the decomposition temperatures of the ESO100 bioplastic were slightly different from those of the ESO57 bioplastic. T_{10}

TABLE II
Decomposition Temperatures of ESO Bioplastics with Different Epoxide Contents

Epoxide content (mol %)	T_5 (°C)	T_{10} (°C)	T_{50} (°C)
24	234.78	267.97	393.78
31	239.26	317.08	389.93
35	251.04	321.89	390.79
40	260.44	328.16	390.77
51	279.22	336.34	391.31
57	295.88	337.91	391.19
100	291.39	335.81	392.12

TABLE III
Effect of the Organoclay (OTAC) Content on the Tensile Properties and Tear Strength of the ESO40 Nanocomposites with 60-pphr MTHPA Cured at 150°C for 75 min

Organoclay content (wt %)	Modulus (MPa)	Tensile strength (MPa)	Elongation at break (%)	Tear strength (N/mm)
0	2.74 ± 0.29	1.33 ± 0.14	78 ± 6	2.18 ± 0.19
1	3.22 ± 0.32	1.52 ± 0.15	71 ± 7	2.29 ± 0.18
3	4.83 ± 0.42	2.18 ± 0.19	74 ± 6	3.53 ± 0.20
5	9.73 ± 0.96	2.90 ± 0.32	80 ± 5	4.11 ± 0.18
8	8.30 ± 1.17	2.87 ± 0.33	76 ± 3	5.28 ± 0.20

could be categorized into three levels: less than 300°C, 300–330°C, and greater than 330°C. No enhancement of thermal decomposition at T_{50} due to epoxide content was derived. It is common for typical polymers that thermal decomposition generally starts at 300°C. Because these ESO bioplastics were crosslinked polymers, their backbone structures were comprised of short-chain hydrocarbons, which were triglycerides. As a result, their thermal decomposition temperatures were relatively low compared with other thermosetting plastics, that is, epoxy. However, the crosslink density in the ESO bioplastics may have increased the service temperature because of the increase in T_5 with epoxide content.

It is difficult to make a comparison of the mechanical properties and characteristics among thermosetting plastics because they are strongly dependent on chemical composition and curing conditions. For example, the mechanical properties of the ESO100 bioplastic listed in Tables I and III (0 wt % organoclay) were different because of different MTHPA contents and different curing times and temperatures. The ESO100 bioplastic prepared by Uyama et al.[35] showed tensile properties as follows: modulus = 11 MPa, tensile strength = 1.4 MPa, and elongation at break = 16%, and these values were lower than ours, which may have been due to the much lower T_g of their sample.

Li and Larock[13] reported the tensile properties of SO–styrene thermosetting copolymers. They found that the tensile properties strongly depended on the styrene content and type of curing agent. For example, with divinyl benzene as a curing agent, the modulus, tensile strength, elongation at break, and tensile toughness were 225 MPa, 11.5 MPa, 40.5%, and 4.00 MPa, respectively, whereas the sample cured with dicumyl peroxide showed a very low modulus (6 MPa), tensile strength (0.3 MPa), and tensile toughness (0.11 MPa) but a higher elongation at break (60.1%). On the basis of a similar T_g, this study showed a lower modulus and a similar tensile strength. This was not unexpected because polystyrene increased modulus of the copolymer because of the rigid benzene ring structure, whereas these ESO bioplastics were composed of only a hydrocarbon backbone. Additionally, this study used a higher testing speed (50 mm/min), whereas Li and Larock[13] used a speed of 5 mm/min. A different testing speed provides a different modulus. The elongation at break of these ESO bioplastics was in the same range as those copolymers.

Tensile properties and characteristics of the ESO nanocomposites

Before we selected Bengel 434 and OTAC, a preliminary study was performed to determine the dispersion of organoclays in ESO and chloroform. Other organoclays, including those in the Bentone family, that is, Bentone SD1, Bentone SD2, Bentone SD3, Bentone SD34, and Bentone SD38, and dioctadecyl trimethyl ammonium bentonite were used. Bengel 434 and OTAC were the most appropriate for ESO100 and ESO40, respectively. ESO sheets containing 51 mol % or greater frequently cracked in the mold after curing, and it was difficult to remove from the mold. Because of the ease of sheet preparation, ESO40 was selected for comparison with ESO100.

Figure 6 shows the stress–strain curves of ESO40 nanocomposites containing clay contents from 1 to 8 wt %. The tensile behavior was similar to that of the

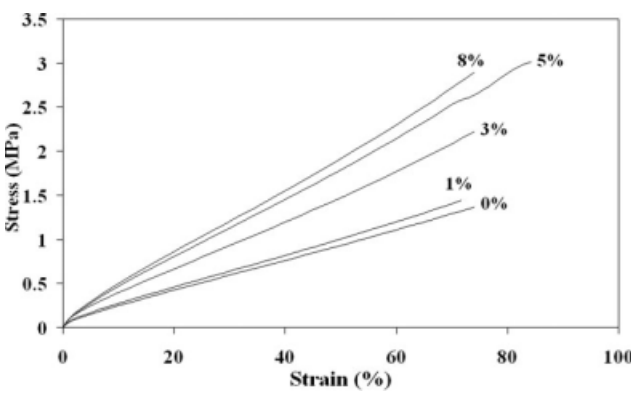

Figure 6 Stress–strain curves of ESO40–organoclay nanocomposites with different organoclay contents.

TABLE IV
Effect of the Organoclay (Bengel 434) Content on the Tensile Properties and Tear Strength of the ESO100 Nanocomposites with 40-pphr MTHPA Cured at 135°C for 60 min

Organoclay content (wt %)	Modulus (MPa)	Tensile strength (MPa)	Elongation at break (%)	Tear strength (N/mm)
0	9.73 ± 1.97	1.68 ± 0.29	33 ± 2	3.73 ± 0.45
1	11.96 ± 1.92	2.14 ± 0.16	33 ± 3	6.05 ± 0.69
3	15.91 ± 1.22	1.73 ± 0.31	22 ± 4	4.08 ± 0.50

ESO bioplastics, with brittle fracture and no yield point. No changes in the stress–strain curves after the organoclay was loaded were observed. The tensile behavior looked similar to soft rubbery materials. The stress increased almost linearly with the strain until failure, which corresponded to the elasticity. Obviously, tensile toughness (area under the stress–strain curves) increased with increasing OTAC content. The stress–strain curves shown in Figure 6 were similar to those reported by Uyama et al.[35]

The effects of various OTAC contents on the tensile properties and the tear resistances of the ESO40 bioplastics are summarized in Table III. The organoclay increased the modulus, tensile strength, and tear resistance and showed little effect on the elongation at break; this was similar to the results reported by Uyama et al.[35] The mechanical properties of the ESO40 nanocomposites depended highly on the organoclay content. The 5 wt % organoclay exhibited the highest tensile properties, whereas the highest tear strength was derived from the 8 wt % organoclay. The modulus increased from 2.74 to 9.73 MPa with increasing organoclay content from 0 to 5 wt %. Similarly, the tensile strength increased from 1.33 to 2.90 MPa with increasing organoclay content from 0 to 5 wt %. However, it should be noted that the elongation at break did not show much difference among these samples. The tear strength also increased twofold after the organoclay was loaded from 0 to 8 wt %. Generally, there is an optimal content for the loading of reinforcing fillers. The lower tensile properties in the sample containing 8 wt % organoclay compared with the sample containing 5 wt % organoclay were probably due to the agglomeration of organoclay in the 8 wt % organoclay sample. These indicated the improvement in the mechanical properties by the incorporation of organoclay into the ESO bioplastics.

To obtain a good molded sheet of the ESO100 bioplastic, only a maximum of 3 wt % Bengel 434 could be used. At higher contents, 5 and 8 wt %, a good dispersion of the mixture was still obtained, but a wrinkled surface appeared on the molded sheets, which resulted in unacceptable tensile specimens. The tensile properties and tear strength of the ESO100 nanocomposites are listed in Table IV. Organoclay increased the modulus, tensile strength, and tear resistance. The effect of the organoclay content on these properties was different in manner. The modulus increased from 9.73 to 15.91 MPa with increasing organoclay content from 0 to 3 wt %, whereas the tensile strength increased slightly after the addition of organoclay. The elongation at break did not change after 1 wt % organoclay was loaded but became lower when the organoclay content was 3 wt %. Although the tear strength was highest at 1 wt % loading, all of the values were in the same range. The effect of the organoclay content seemed to be superior in the modulus, whereas the other properties showed insignificant changes. Keep in mind that the chemical composition and curing conditions of the samples shown in Table IV were different from those of the ESO100 bioplastic shown in Table I.

The mechanical property most improved by the addition of organoclay in both the ESO100 bioplastic and the ESO40 bioplastic was the increased modulus. The organoclays did not deteriorate the elongation at break of these bioplastics. The lower values of modulus and tensile strength at 8 wt % organoclay content were attributed to the inevitable aggregation of the organoclay. The ESO100 nanocomposite revealed a higher tensile modulus and tear strength than the ESO40 nanocomposite, but the tensile strength of both ESO nanocomposites was in the same range. The higher elongation at break in the ESO40 nanocomposites resulted from fewer functional groups, which led to a lower crosslink density in the polymer matrix. The tensile strength and modulus of the ESO100 bioplastic and ESO100 nanocomposite of this study were higher than those reported by Liu et al.[36] They used triethylenetetramine and Cloisite 30B as a curing agent and reinforcing organoclay, respectively. This was probably due to the higher T_g of this nanocomposite and the different type of organoclay.

The effect of the organoclay (OTAC) content on E' of the ESO40 nanocomposites is displayed in Figure 7. E', including the modulus at the rubbery plateau

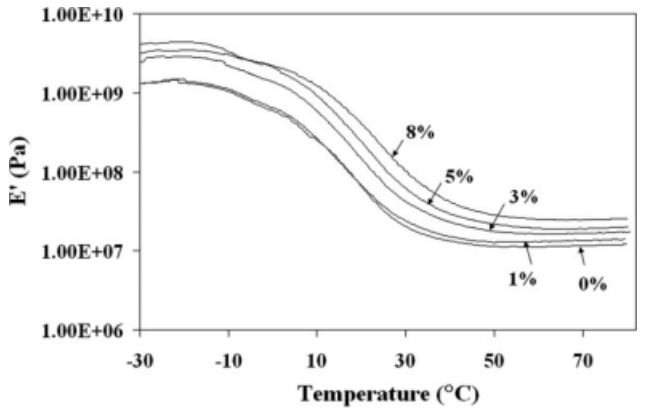

Figure 7 *E′*–temperature curves of ESO40–organoclay nanocomposites with different organoclay contents.

region, increased as the organoclay content increased from 0 to 8 wt %. All of the samples showed a broad transition from the glassy to the rubbery state, similar to the ESO bioplastics. The T_g received from the maximum tan δ peak is listed in Table V. No significant changes in T_g were found in the samples containing 3 wt % or lower OTAC. A remarkable enhancement in T_g, from 30.3 to 36.3°C, was illustrated in the sample containing 8 wt % OTAC. The effect of OTAC content on the thermal degradation of the ESO40 nanocomposites is revealed in Table V. OTAC increased the thermal degradation resistance, and the optimum value was in the sample containing 5 wt % OTAC. With further increases OTAC content (8 wt %), the decomposition temperatures (T_5, T_{10}, and T_{50}) decreased close to those of the sample without organoclay (0 wt % OTAC). The maximum increase in thermal stability was approximately 20–30°C. It was established that the well-dispersed layered silicate in the exfoliated nanocomposites acted as barriers to prevent oxidation when heated in air, whereas the intercalated structure of the layered silicate showed relatively poor thermal properties. It is essential to remark that the thermal decomposition experiment was carried out in nitrogen. Therefore, there was not much improvement in the thermal stability, similar to that reported by Liu et al.[36]

TABLE V
T_g's and Decomposition Temperatures of ESO40 Nanocomposites with Different Organoclay Contents

OTAC content (mol %)	T_g (°C)[a]	T_5 (°C)	T_{10} (°C)	T_{50} (°C)
0	30.3	222.80	272.36	382.24
1	29.6	223.42	281.42	388.93
3	31.6	231.48	290.94	390.21
5	33.6	241.48	299.69	390.13
8	36.3	221.29	267.49	387.67

[a] Temperature at the maximum tan δ peak.

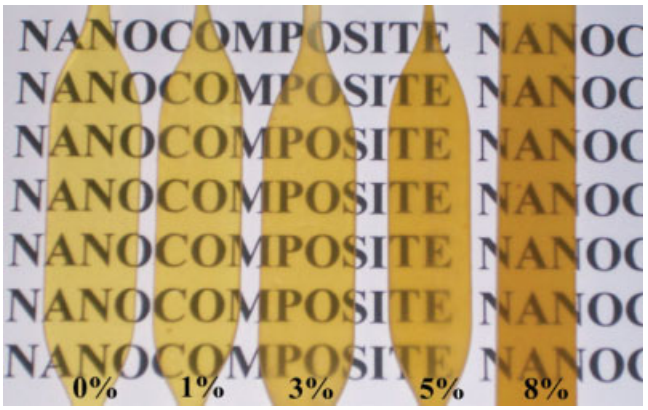

Figure 8 Photograph of ESO40–organoclay nanocomposites with 1–8 wt % OTAC. [Color figure can be viewed in the online issue, which is available at www.interscience.wiley.com.]

The sample without organoclay was amber in color and transparent. After the introduction of the organoclay, the color became darker, and the transparency decreased with increasing organoclay content. The transparency of all of these ESO nanocomposites was so high that it was able to read letters placed underneath the samples (Fig. 8). This appearance indicated good dispersion, and few aggregates of organoclay stacks were achieved. Figure 9 shows

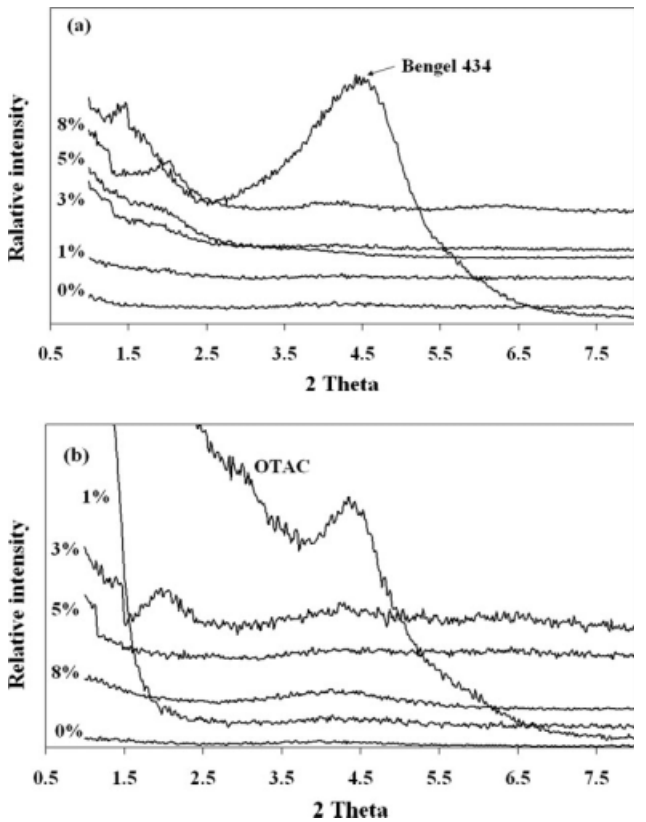

Figure 9 XRD patterns of ESO–organoclay nanocomposites with different organoclay contents: (a) ESO100 mixed with Bengel 434 and (b) ESO40 mixed with OTAC.

the wide-angle X-ray diffraction (XRD) patterns of the organoclays (Bengel 434 and OTAC) and ESO nanocomposites with different clay contents. Bengel 434 and OTAC showed clear peaks at $2\theta = 4.50$ and 4.39°, which were attributed to the (001) plane (d_{001}) with a mean interlayer spacing of 19.61 and 20.10 Å, respectively. There were no clear peaks in either the ESO100 nanocomposite or the ESO40 nanocomposite containing 1 wt % organoclay; this indicated the destruction of the regular layered silicate. On the basis of these XRD patterns, exfoliation occurred in both ESO nanocomposites. However, characterization by TEM was necessary to verify this conclusion. There was a very broad peak (hump) at $2\theta = 1.90°$ in the samples containing 3 and 5 wt % Bengel 434 and one sharp peak at $2\theta = 2.00°$ in the sample containing 8 wt % Bengel 434. The samples containing 3 wt % OTAC showed a peak at $2\theta = 1.98°$, whereas the others showed no clear peaks. The *d*-spacing at d_{001} calculated with Bragg's equation is tabulated in Table VI; it suggested the intercalation of organoclay due to the enhancement of *d*-spacing. Because of XRD analysis, the ESO nanocomposites were derived in this study.

The morphology of the ESO nanocomposites was observed by TEM and is shown in Figure 10. The dark lines in the figures corresponded to the silicate layers. No aggregation of organoclay particles was observed; this suggested good dispersion of the organoclay particles in the ESO matrix, as mentioned earlier with regard to the transparency of samples. The ESO100 nanocomposite containing 3 wt % Bengel 434 [Fig. 10(a)] exhibited oriented silicate layers (intercalation) and partly unoriented layers (exfoliation); therefore, a very broad peak at the lower 2θ was observed in the XRD pattern. The dispersion of 1 wt % OTAC in the ESO40 nanocomposite [Fig. 10(b)] showed relatively more unoriented silicate layers. All of the samples showed a similar intercalated structure, as shown in Figure 10. It was unambiguous that intercalation took place in these ESO nanocomposites.

TABLE VI
***d*-Spacing of Organoclays in the ESO Nanocomposites**

Sample	*d*-Spacing at d_{001} (Å)
Bengel 434	19.61
ESO100 + 1% Bengel 434	—
ESO100 + 3% Bengel 434	46.69
ESO100 + 5% Bengel 434	46.69
ESO100 + 8% Bengel 434	44.12
OTAC	20.10
ESO40 + 1% OTAC	—
ESO40 + 3% OTAC	44.57
ESO40 + 5% OTAC	—
ESO40 + 8% OTAC	—

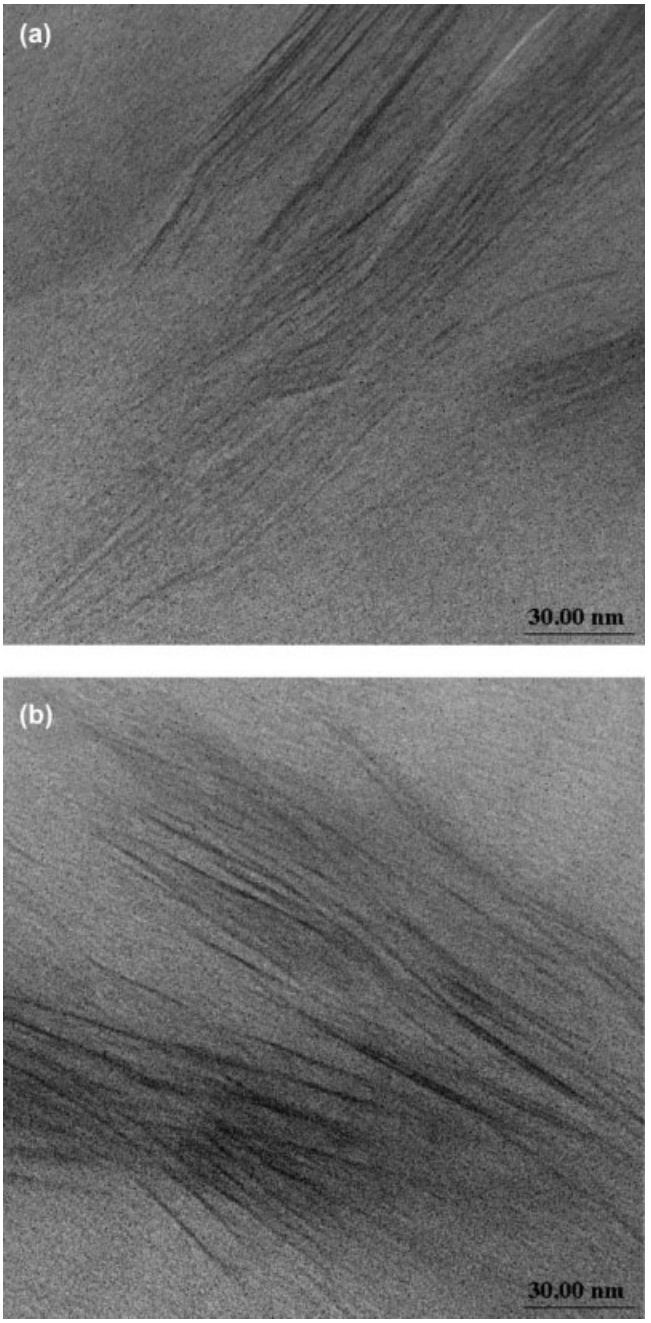

Figure 10 TEM micrographs of ESO–organoclay nanocomposites: (a) ESO100 and 3% Bengel 434 and (b) ESO40 and 1% OTAC.

CONCLUSIONS

ESO bioplastics with various epoxide contents were prepared. As the epoxide content increased, more reactive groups were derived, which led to a higher crosslink density after curing with MTHPA. Therefore, the modulus, tensile strength, tear resistance, T_g, and thermal stability increased with increasing epoxide content. In contrast, the elongation at break showed no trend for samples containing epoxide contents from 31 to 88 mol %. The ESO

nanocomposites were derived by the choice of an appropriate organoclay for each ESO. Improvements in the properties were attained at relatively low organoclay contents ($\leq$5 wt %). The Young's modulus, tensile strength, and tear resistance increased with organoclay content, whereas no significant change in the elongation at break was observed. T_g significantly increased only in the sample containing 8 wt % organoclay. XRD and TEM analysis exhibited intercalation in these ESO nanocomposites. All samples showed an intercalation structure, and only the sample containing 1 wt % OTAC displayed a slight exfoliation structure. The thermal stability of the ESO nanocomposites did not improve much because of the occurrence of a mainly intercalated structure of the nanocomposites and with a nitrogen atmosphere in the experiment. This study showed the accomplishment of the synthesis of ESO with various epoxide contents that provided more toughness than commercial ESO100 and also showed success in the preparation of *in situ* intercalated ESO nanocomposites.

The authors are grateful to Pensri Promrat and Duangruthai Srinun for their assistance with the experiments. They are also grateful to Toemsak Srikirin (Mahidol University) for his organoclay support and to Arkema, Inc. (Philadelphia, PA), and Sritepthai Co., Ltd. (Thailand), for their Vikoflex 7170 support. The authors appreciate Toemsak Srikirin for his helpful suggestions.

References

1. Carole, T. M.; Pellegrino, J.; Paster, M. D. Appl Biochem Biotechnol 2004, 115, 871.
2. Eckwert, K. U.S. Pat.4,647,678 (1987).
3. Mulder, A. J. U.S. Pat.4,721,798 (1987).
4. Meffert, A.; Kluth, H. U.S. Pat.4,886,893 (1988).
5. Park, S. J.; Jin, F. L.; Lee, J. R. Macromol Rapid Commun 2004, 25, 724.
6. Campanella, A.; Baltanas, M. A. J Lipid Sci Technol 2004, 106, 524.
7. Campanella, A.; Baltanas, M. A. Chem Eng J 2006, 18, 141.
8. Guo, Y.; Hardesty, J. H.; Mannari, V. M. J Am Oil Chem Soc 2007, 84, 929.
9. Lin, B.; Yang, L.; Dai, H.; Yi, A. J Am Oil Chem Soc 2008, 85, 113.
10. Adhvaryu, A.; Erhan, S. Z. Ind Crops Prod 2002, 15, 247.
11. Hwang, H. S.; Erhan, S. E. Ind Crops Prod 2006, 23, 311.
12. Li, F.; Larock, R. C. J Appl Polym Sci 2001, 80, 658.
13. Li, F.; Larock, R. C. J Polym Sci Part B: Polym Phys 2001, 39, 60.
14. Can, E.; Küsefoğlu, S.; Wool, R. P. J Appl Polym Sci 2001, 81, 69.
15. Holser, R. A. Ind Crops Prod 2008, 27, 130.
16. González-Ortiz, L. J.; Arellano, M.; Sanchez-Pena, M. J. Polym Degrad Stab 2006, 91, 2715.
17. Thames, S. F.; Yu, H. Surf Coat Technol 1999, 115, 208.
18. Gu, H.; Ren, K.; Dustin, M. J Coat Technol 2002, 74, 49.
19. Giddings, C. L.; Trumbo, D. L. Prog Org Coat 1997, 30, 219.
20. Raghavachar, R.; Sarnecki, G.; Baghdachi, J. J Coat Technol 2000, 72, 125.
21. Mohamed, H. A.; Badran, B. M.; Aglan, H. A. J Appl Polym Sci 2001, 80, 286.
22. John, J.; Bhattacharya, M.; Turner, R. B. J Appl Polym Sci 2002, 86, 3097.
23. Konii, S. U.S. Pat.4,209,429 (1980).
24. Yue, Z.; Jianfeng, H.; Hang, H. Chin J Chem Eng 2007, 15, 418.
25. Park, S. J.; Jin, F. L.; Lee, J. R. Mater Sci Eng Part A 2004, 374, 109.
26. Zhu, J.; Chandrashekhara, K.; Flanigan, V.; Kapila, S. J Appl Polym Sci 2004, 91, 3513.
27. Miyagawa, H.; Misra, M.; Drzal, L. T.; Mohanty, A. K. Polym Eng Sci 2005, 45, 487.
28. Liu, Z. S.; Erhan, S. Z.; Calvert, P. D. Compos A 2007, 38, 87.
29. Jin, F. L.; Park, S. J. Mater Sci Eng Part A 2008, 478, 402.
30. Lu, J.; Knot, S.; Wool, R. P. Polymer 2005, 46, 71.
31. Lu, J.; Wool, R. P. Polym Eng Sci 2007, 47, 1469.
32. Xu, J.; Liu, Z.; Erhan, S. Z.; Carriere, C. J. J Am Oil Chem Soc 2004, 81, 813.
33. Xu, J.; Liu, Z.; Erhan, S. Z. J Am Oil Chem Soc 2008, 85, 285.
34. Deffar, D.; Teng, G.; Soucek, M. D. Macromol Mater Eng 2001, 286, 204.
35. Uyama, H.; Kuwabara, M.; Tsujimoto, T.; Nakano, M.; Usuki, A.; Kobayashi, S. Macromol Biosci 2004, 4, 354.
36. Liu, Z. S.; Erhan, S. Z.; Xus, J. Polymer 2005, 46, 10119.
37. Song, B.; Weinong, C.; Zengshe, L.; Sevim, E. Int J Plast 2006, 22, 1549.
38. Liu, Z. S.; Erhan, S. Z. Mater Sci Eng Part A 2008, 483, 708.
39. Lu, J.; Wool, R. P. Compos Sci Technol 2008, 68, 1025.
40. Khot, S. N.; Lascala, J. J.; Erde, L.; Can, E.; Morye, S. S.; Williams, G. I.; Palmese, G. R.; Usefoglu, S. H.; Wolm, R. P. J Appl Polym Sci 2001, 82, 703.
41. Knoth, G. J Am Oil Chem Soc 2001, 77, 489.
42. Knoth, G.; Kenar, J. A. Eur J Lipid Sci Technol 2004, 106, 88.
43. Igarashi, T.; Aursand, M.; Hirata, Y.; Gribbestad, I. S.; Wada, S.; Nonaka, M. J Am Oil Chem Soc 2000, 77, 737.